J. Braz. Chem. Soc., Vol. 8, No. 6, 641-647, 1997.
Printed in Brazil.

0103 – 5053 $6.00 + 0.00

Article

Synthesis, Characterization and Molecular Structures of the Pyridinium *trans*-Bis(pyridine)tetrachlororuthenate(III) and Pyridinium *trans*-(carbonyl)(pyridine)tetrachlororuthenate(III)

Alzir A. Batista[a*], Sandra A. Onofre[a], Salete L. Queiroz[a], Glaucius Oliva[b], Marcos R.M. Fontes[b,c], and Otaciro R. Nascimento[b]

[a]*Departamento de Química, Universidade Federal de São Carlos, C.P. 676, 13565-905 São Carlos - SP, Brazil*

[b]*Instituto de Física de São Carlos, Universidade de São Paulo, C.P. 369, 13560-970 São Carlos - SP, Brazil*

[c]*Departamento de Física e Biofísica, IB-UNESP, C.P. 510, 18618-000 Botucatu - SP, Brazil*

Received: April 7, 1997

Os complexos pyH[*trans*-$RuCl_4(py)_2$](**1**) and pyH[*trans*-$RuCl_4(CO)(py)$](**2**) foram sintetizados e cristalizam-se no grupo espacial $P2_1/n$, Z = 4 com a = 8.080(7), b = 22.503(7), c = 10.125(6) Å, β = 93.19(6)° para (**1**) e a = 7.821(1), b = 10.337(3), c = 19.763(3) Å, β = 93.07(1)° para (**2**). As estruturas foram resolvidas pelas técnicas de Patterson e diferenciais de Fourier e refinadas para R = 0.062 para (**1**) e R = 0.038 para (**2**). Em ambos os casos o Ru(III) encontra-se octaédricamente coordenado a quatro átomos de cloro, ao nitrogênio do anel piridínico ou ao carbono do monóxido de carbono. Outro grupo piridínico protonado, o qual forma o cátion, completa as estruturas cristalinas. Os espectros de absorção na região do UV-Vis apresentam três bandas: (**1**) 360 (ε = 1180 M^{-1} cm^{-1}), 441 (ε = 3200 M^{-1} cm^{-1}) e 532 nm (ε = 400 M^{-1} cm^{-1}); (**2**) 315(ε = 1150 M^{-1} cm^{-1}), 442 (ε = 3170 M^{-1} cm^{-1}) e 530 nm (ε = 390 M^{-1} cm^{-1}). As duas bandas de energias mais altas foram associadas com transições de transferência de ligante → metal e a terceira banda, de mais baixa energia foi atribuída à transição d-d. Espectro de RPE a baixa temperatura confirmou a presença de Ru(III) paramagnéticamente ativo e é consistente com uma simetria axial para os complexos. A posição da banda de estiramento CO no complexo (**2**) é discutida em termos da retrodoação metal-CO.

The pyH[*trans*-$RuCl_4(py)_2$](**1**) and pyH[*trans*-$RuCl_4(CO)(py)$](**2**) complexes were synthesized and found to crystallize in space group $P2_1/n$, Z = 4 with a = 8.080(7), b = 22.503(7), c = 10.125(6) Å, β = 93.19(6)° for (**1**) and a = 7.821(1), b = 10.337(3), c = 19.763(3) Å, β = 93.07(1)° for (**2**). The structures were solved by Patterson and difference Fourier techniques and refined to R = 0.062 for (**1**) and R = 0.038 for (**2**). In both cases the Ru(III) ion is octahedrally coordinated to four co-planar chlorine atoms, the nitrogen of the pyridine rings or carbon from the carbon monoxide. Another protonated pyridine group, which forms the counter-cation completes the crystal structures. The UV-Vis absorption spectra show three bands: (**1**) 360 (ε = 1180 M^{-1} cm^{-1}), 441 (ε = 3200 M^{-1} cm^{-1}) and 532 nm (ε = 400 M^{-1} cm^{-1}); (**2**) 315(ε = 1150 M^{-1} cm^{-1}), 442 (ε = 3170 M^{-1} cm^{-1}) and 530 nm (ε = 390 M^{-1} cm^{-1}). The two higher energy bands were associated with ligand-to-metal

charge transfer transitions and a third band at lower energy was assigned to a d-d transition. Low temperature EPR data confirmed the presence of the paramagnetically active Ru(III) and it is consistent with axial symmetry of the complexes. The position of the stretching CO band in complex (**2**) is discussed in terms of metal-CO backbonding.

Keywords: *ruthenium, tetrachlororuthenate(III), X-ray structures*

Introduction

During the last 30 years, since cis-diaminedichloroplatinum(II) was discovered as a potent tumor-inhibiting agent, intense research activity has been devoted to the field of antitumor-active metal complexes[1]. Most of these efforts were concentrated on platinum as the central metal. Many platinum complexes were synthesized and more than a thousand were investigated in preclinical tests for antitumor activity. Furthermore it was clearly demonstrated that the relatively close pharmacological and toxicological behavior of most of these new derivatives compared well with the original cisplatin. Owing to these facts, it is necessary to search for non-platinum complexes, which may also exhibit tumor-inhibiting properties. So the development of complexes as an alternative to platinum metal inhibitors is of special interest and ruthenium compounds have been studied extensively for this purpose[2,3]. A few years ago the ImH[*trans*-$RuCl_4(Im)_2$] was reported in the literature and its tumor-inhibiting properties were described[4]. This Ru(III) imidazole complex is active against colorectal tumors, reducing the tumor volume to about 20-10% and it is currently undergoing preclinical pharmacological tests[4,5]. It has been reported that it binds to DNA and blocks its template-primer properties in DNA-polymerase catalyzed duplication[6]. Due to the increasing interest in this class of ruthenium(III) complexes , we started recently a research program to search for simple methods of synthesis of this kind of compounds. Consequently, the synthesis and characterization of several new complexes were undertaken[7]. In the present paper we report on the synthesis and characterization of pyH[*trans*-$RuCl_4(py)_2$] and pyH[*trans*-$RuCl_4$(CO)(py)].

Experimental

Solvents for the preparation of the complexes or measurements were chemically pure grade and were dried prior to use.

Preparations

Complex (**1**): pyH[*trans*-$RuCl_4(py)_2$]

Commercial (Degussa) hydrated ruthenium trichloride (0.3 g 1.2 mmol), was dissolved in ethanol (10 mL) and a stream of carbon monoxide was passed through it, for 12 h, at room temperature. The red solution was allowed to stand in contact with air for 24 h and pyridine (7.6 mmol, Merck) dissolved in 3 mL of ethanol/1mL of 8 N HCl was added. The solution was stirred for *ca.* 3 h and the solution was allowed to stand for 2 days at room temperature. The volume of the solution was reduced to about 2 mL and diethyl ether was added to precipitate a red powder (yield 70%) which was filtered off, washed with ethanol and dried in a dessicator over $CaCl_2$. The red powder was recrystalized from dichloromethane/ether affording bright red orange crystals. Calc. for $C_{15}H_{16}N_3Cl_4Ru$: C, 37.44; H, 3.35; N, 8.73%. Found; C, 37.62; H, 3.28, N, 9.00%

Complex (**2**): pyH[*trans*-$RuCl_4$(CO)(py)]

This complex was prepared according to the method previously described in the literature[8] with some modifications. The red solution was obtained as described above. The pyridine (7.6 mmol) dissolved in 3 mL of ethanol was added and the mixture was refluxed for *ca.* 2 h. Addition of diethyl ether gave the complex in the form of an orange powder (yield 80%) which was filtered off, washed with ethanol and dried in dessicator over $CaCl_2$. The powder was recrystalized from dichloromethane/ether affording the product as bright orange crystals. Calc. for $C_{11}H_{11}N_2O_1Cl_4Ru$: C, 30.72; H, 2.58; N, 6.51%. Found: C, 30.70; H, 2.80; N, 6.71%.

X-ray diffraction data

Complete data sets were collected on an Enraf-Nonius CAD-4 four cycle diffractometer, from flat prismatic crystals. Experimental details are given in Table 1. Cell dimensions and the orientation matrices were calculated by least-squares from 25 centered reflections in the range $10 < \theta < 19$ for (**1**) and $7 < \theta < 19°$ for (**2**). Difraction intensities were measured by the $\omega - 2\theta$ scan technique using a variable scan speed of 0.8-5.5° min^{-1} for (**1**) and 1.7-5.5° min^{-1} for (**2**) determined by a pre-scan at 5.5° min^{-1}. The intensity of one standard reflection was essentially constant over the duration of both experiments. Data were corrected for Lorentz, polarization and absorption effects, following the procedure of Walker and Stuart[9].

Crystal structure determination and refinement

The determination and refinement of the structures were performed with the SHELX76[10] system of programs. The structures were solved by standard Patterson and difference Fourier techniques and refined by full-matrix least-squares methods with anisotropic thermal parameters for the non-hydrogen atoms, with the exception of the pyH ring of structure **(2)** which, due to disorder, was refined as a rigid group with isotropic temperature factors for individual atoms. All hydrogen atoms were located on stereochemical grounds and included as fixed contributors with a common isotropic temperature factor of 0.08 $Å^2$, with the exception of the H-atoms of the mobile pyH of structure (2) which were not included. Bonded H-atom scattering factors[11] and complex scattering factors[12] were employed for the remaining atoms. Figure 1a and 1b were drawn with the ORTEP program[13] with all non-H atoms represented with 50% ellipsoids for the anisotropic thermal parameters.

Table 1. Crystal data, data collection details and structure refinement results for pyH[*trans*-$RuCl_4(py)_2$] and pyH[*trans*-$RuCl_4(CO)py$].

Formula	$C_{15}Cl_4H_{16}N_3Ru$	$C_{11}Cl_4H_{11}N_2ORu$
M	481.2	430.11
System	Monoclinic	Monoclinic
Space group	$P2_1/n$	$P2_1/n$
a (Å)	8.080(7)	7.821(1)
b (Å)	22.503(7)	10.337(3)
c (Å)	10.125(6)	19.763(3)
β (°)	93.19(6)	93.07(1)
V ($Å^3$)	1838(2)	1595.5(5)
Z	4	4
D_c (g cm^{-3})	1.739	1.790
λ (Å)	(MoKα) 0.71073	(MoKα) 0.71073
Sample dimensions (mm)	0.05 x 0.30 x 0.60	0.03 x 0.17 x 0.17
Linear absorption coefficient (μ) (cm^{-1})	13.06	14.86
Absorption correction factors	1.16, 0.86	1.21, 0.83
Scan technique	ω – 2θ	ω – 2θ
θ range (°)	0-23	0-25
F(000)	960	848
Reflections measured	2856	5800
Unique reflections	2222	2582
R_{int}	0.03	0.03
Reflections above 3 σ(I)	1553	1478
Minimized function	$\sum w(\lvert F_0\rvert - \lvert F_c\rvert)^2$	$\sum w(\lvert F_0\rvert - \lvert F_c\rvert)^2$
Weighting scheme (w =)	$[\sigma^2\lvert F_0\rvert + 0.0008\lvert F_0\rvert^2]^{-1}$	$[\sigma^2\lvert F_0\rvert + 0.0005\lvert F_0\rvert^2]^{-1}$
R	0.038	0.062
R_w	0.039	0.063
S	1.19	1.88
Range h; k; l	0, 8; 0, 24; -11, 11	-9, 9; -12, 12; 0, 23
Max.	min. residual ρ ($eÅ^{-3}$)	0.59, -0.46

List of H-atom positions, anisotropic thermal parameters and structure factors are available on request from the authors.

Spectroscopic measurements

IR spectra

Pellets were prepared from crystalline powder samples diluted in CsI. Measurements were performed on a Bomem-Michelson 102 spectrometer in the region 4000-200 cm^{-1}.

UV/Vis spectra

The electronic spectra were measured in CH_2Cl_2 solution (8 x 10^{-5} mol/L) on a Varian DMS-100 spectrophotometer.

EPR measurements

EPR spectra were obtained from a polycrystalline powder sample, using a quartz tube, on a Varian E-109 spectrometer equipped with X band bridge at -150 °C Modulation amplitude: 9 gauss. Microwave power: 10 mW.

Magnetic susceptibility

Solution magnetic susceptibilities were measured by the Evans NMR method[14], with a 200 MHz Bruker instrument, using CD_2Cl_2 solution at room temperature.

Electrical conductivity

Solution electrical conductivities were measured in nitromethane at 25 °C under anaerobic conditions using a Micronal conductivity bridge.

Results and Discussion

Selected interatomic bond distances are in Table 2 and interatomic angles are in Table 3. Final atomic parameters for non-H atoms are given in Table 4 and Table 5. Figure 1a and 1b are drawings of the complex pyH[trans-$RuCl_4(py)_2$] (**1**) and trans-pyH[*trans*-$RuCl_4(CO)(py)$](**2**), respectively. In complex (**1**) the Ru(III) ion is octahedrally coordinated to four coplanar chlorine atoms and two nitrogen atoms of the pyridine rings *trans* to each other. In complex (**2**) the Ru(III) ion is also octahedrally coordinated to four coplanar chlorine atoms and to the carbon atom of a CO group *trans* to a nitrogen of the pyridine ring. In both cases a protonated pyridine molecule is electrostatically bonded to the negatively charged Ru(III) complex, completing the crystal structures of the compounds.

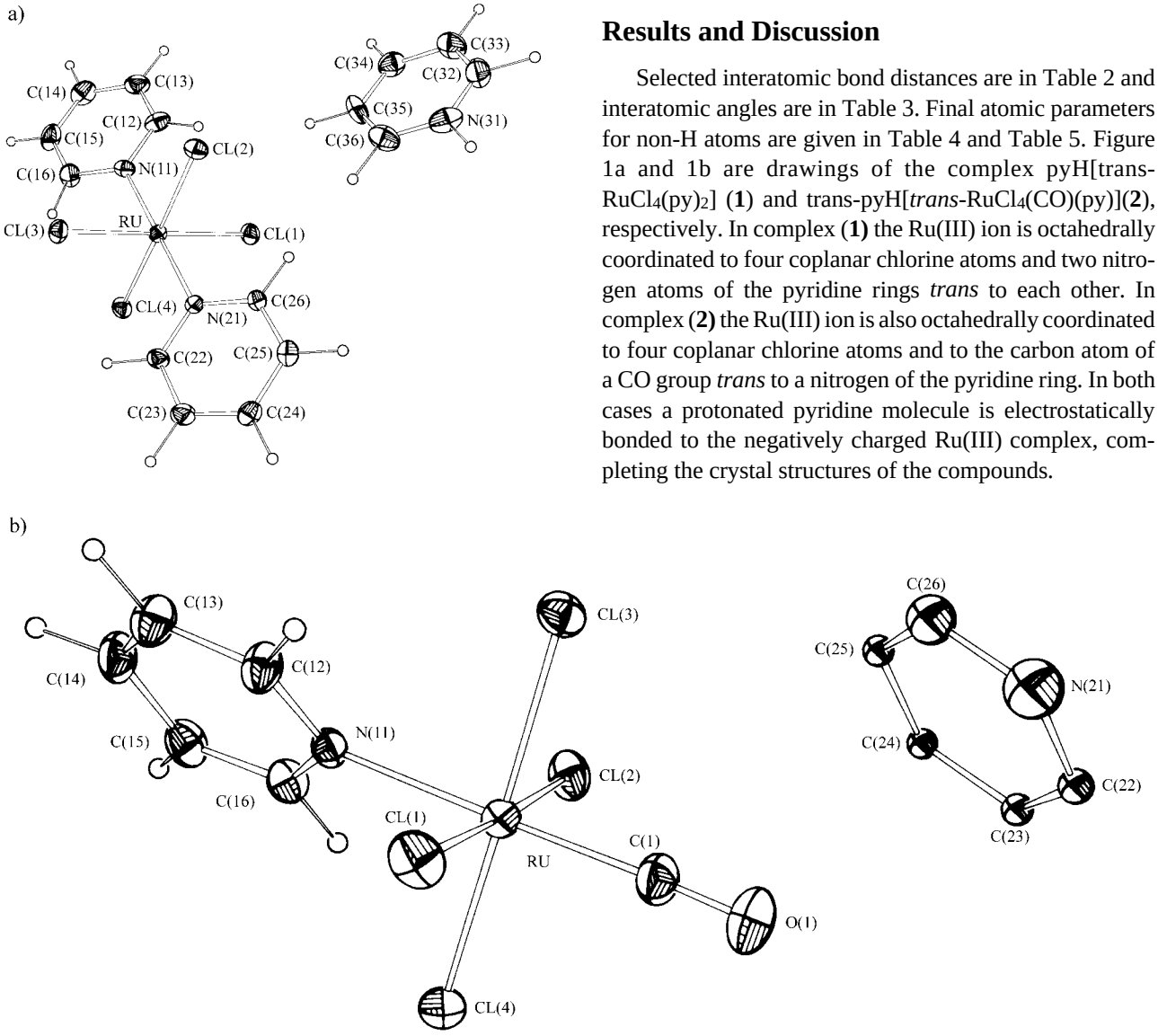

Figure 1. ORTEP drawings of pyH[*trans*-$RuCl_4(py)_2$] (a), and pyH[*trans*-$RuCl_4(CO)(py)$] (b).

Table 2. Selected bond distances (Å) for pyH[*trans*-$RuCl_4(py)_2$] and pyH[*trans*-$RuCl_4(CO)(py)$].

pyH[*trans*-$RuCl_4(py)_2$]			
Ru	-	Cl(1)	2.356(2)
Ru	-	Cl(2)	2.357(2)
Ru	-	Cl(3)	2.356(2)
Ru	-	Cl(4)	2.343(2)
Ru	-	N(11)	2.078(8)
Ru	-	N(21)	2.086(7)
N(11)	-	C(12)	1.34(1)
N(11)	-	C(16)	1.36(1)
C(12)	-	C(13)	1.40(2)
C(13)	-	C(14)	1.38(2)
C(14)	-	C(15)	1.36(2)
C(15)	-	C(16)	1.37(2)
N(21)	-	C(22)	1.34(1)
N(21)	-	C(26)	1.35(1)
C(22)	-	C(23)	1.38(1)
C(23)	-	C(24)	1.38(1)
C(24)	-	C(25)	1.39(1)
C(25)	-	C(26)	1.40(1)
N(31)	-	C(32)	1.31(1)
N(31)	-	C(36)	1.31(1)
C(32)	-	C(33)	1.33(2)
C(33)	-	C(34)	1.35(2)
C(34)	-	C(35)	1.36(2)
C(35)	-	C(36)	1.38(2)
pyH[*trans*-$RuCl_4(CO)py$]			
Ru	-	Cl(1)	2.329(4)
Ru	-	Cl(2)	2.349(4)
Ru	-	Cl(3)	2.360(4)
Ru	-	Cl(4)	2.332(4)
Ru	-	C(1)	1.87(2)
Ru	-	N(11)	2.14(1)
O(1)	-	C(1)	1.11(2)
N(11)	-	C(12)	1.34(2)
N(11)	-	C(16)	1.34(2)
C(12)	-	C(13)	1.39(2)
C(13)	-	C(14)	1.34(2)
C(14)	-	C(15)	1.42(2)
C(15)	-	C(16)	1.36(2)
N(21)	-	C(22)	1.40(2)
N(21)	-	C(26)	1.40(2)
C(22)	-	C(23)	1.40(2)
C(23)	-	C(24)	1.39(2)
C(24)	-	C(25)	1.39(2)
C(25)	-	C(26)	1.40(2)

The Ru-Cl and Ru-N bond lengths in the complexes **(1)** [2.353(2) and 2.082(8) Å] and **(2)** [2.342(4) and 2.14(1) Å], respectively are comparable to those found for similar complexes: ImH[*trans*-$RuCl_4(Im)_2$] complex [2.349(1)

Table 3. Selected interatomic angles (Å) for pyH[*trans*-$RuCl_4(py)_2$] and pyH[*trans*-$RuCl_4(CO)(py)$].

pyH[*trans*-$RuCl_4(py)_2$]					
Cl(1)	-	Ru	-	Cl(2)	- 88.4(2)
Cl(1)	-	Ru	-	Cl(3)	- 179.1(2)
Cl(1)	-	Ru	-	Cl(4)	- 90.7(2)
Cl(1)	-	Ru	-	N(11)	- 90.4(4)
Cl(1)	-	Ru	-	N(21)	- 89.3(5)
Cl(2)	-	Ru	-	Cl(3)	- 90.7(2)
Cl(2)	-	Ru	-	Cl(4)	- 178.9(2)
Cl(2)	-	Ru	-	N(11)	- 90.4(4)
Cl(2)	-	Ru	-	N(21)	- 91.4(5)
Cl(3)	-	Ru	-	Cl(4)	- 90.2(2)
Cl(3)	-	Ru	-	N(11)	- 89.8(4)
Cl(3)	-	Ru	-	N(21)	- 90.6(5)
Cl(4)	-	Ru	-	N(11)	- 90.2(4)
Cl(4)	-	Ru	-	N(21)	- 88.0(5)
N(11)	-	Ru	-	N(21)	- 178.1(6)
Ru	-	N(11)	-	C(12)	- 119(1)
Ru	-	N(11)	-	C(16)	- 122(1)
Ru	-	N(21)	-	C(22)	- 120(1)
Ru	-	N(21)	-	C(26)	- 125(1)
pyH[*trans*-$RuCl_4(CO)(py)$]					
Cl(1)	-	Ru	-	Cl(2)	- 177.4(1)
Cl(1)	-	Ru	-	Cl(3)	- 89.4(1)
Cl(1)	-	Ru	-	Cl(4)	- 90.7(1)
Cl(1)	-	Ru	-	C(1)	- 90.6(5)
Cl(1)	-	Ru	-	N(11)	- 88.9(3)
Cl(2)	-	Ru	-	Cl(3)	- 89.1(1)
Cl(2)	-	Ru	-	Cl(4)	- 90.8(1)
Cl(2)	-	Ru	-	C(1)	- 91.5(5)
Cl(2)	-	Ru	-	N(11)	- 89.0(3)
Cl(3)	-	Ru	-	Cl(4)	- 179.3(1)
Cl(3)	-	Ru	-	C(1)	- 89.5(5)
Cl(3)	-	Ru	-	N(11)	- 89.4(3)
Cl(4)	-	Ru	-	C(1)	- 91.2(5)
Cl(4)	-	Ru	-	N(11)	- 89.9(3)
C(1)	-	Ru	-	N(11)	- 178.7(6)
Ru	-	C(1)	-	O(1)	- 178(1)

Table 4. Fractional Atomic coordinates and isotropic temperature parameters ($Å^2$)for pyH[*trans*-$RuCl_4(py)_2$].

Atom	X/A	Y/B	Z/C	Biso
Ru	0.1842(1)	0.0972(0)	0.2561(1)	2.66(2)
Cl1	0.4254(3)	0.1551(1)	0.2414(2)	3.81(8)
Cl2	0.2626(3)	0.0697(1)	0.4754(2)	3.96(8)
Cl3	-0.0570(3)	0.0396(1)	0.2743(2)	3.80(8)
Cl4	0.1017(3)	0.1238(1)	0.0386(2)	3.92(8)
N11	0.0595(9)	0.1711(3)	0.3234(7)	3.3(3)
N21	0.3087(8)	0.0235(3)	0.1856(7)	2.9(3)
N31	0.863(2)	0.0780(4)	0.622(1)	5.7(4)
C12	0.129(1)	0.2080(5)	0.415(1)	4.7(4)
C13	0.049(2)	0.2590(5)	0.457(1)	5.4(5)
C14	-0.108(2)	0.2716(5)	0.405(1)	5.8(5)
C15	-0.178(1)	0.2342(5)	0.313(1)	5.7(5)
C16	-0.095(1)	0.1846(4)	0.273(1)	4.5(4)
C22	0.238(1)	-0.0110(4)	0.0904(9)	3.4(3)
C23	0.320(1)	-0.0588(5)	0.038(1)	4.3(4)
C24	0.478(1)	-0.0732(4)	0.086(1)	3.9(4)
C25	0.551(1)	-0.0379(5)	0.186(1)	4.0(4)
C26	0.463(1)	0.0104(5)	0.2338(8)	3.6(3)
C32	0.935(2)	0.1160(7)	0.705(1)	6.2(5)
C33	0.878(2)	0.1710(6)	0.721(1)	6.0(5)
C34	0.738(2)	0.1863(5)	0.651(1)	5.5(5)
C35	0.660(2)	0.1480(7)	0.565(1)	6.5(5)
C36	0.726(2)	0.0916(6)	0.554(1)	6.0(5)

Table 5. Fractional Atomic coordinates and isotropic temperature parameters ($Å^2$)for pyH[*trans*-$RuCl_4$(CO)py].

Atom	X/A	Y/B	Z/C	Biso
Ru	0.2014(1)	0.2772(1)	0.3929(1)	3.60(4)
Cl(1)	0.4657(5)	0.2656(4)	0.3442(2)	5.7(2)
Cl(2)	-0.0585(4)	0.2904(4)	0.4468(2)	5.1(1)
Cl(3)	0.2791(5)	0.4806(3)	0.4392(2)	4.5(1)
Cl(4)	0.1253(5)	0.0750(4)	0.3485(2)	5.6(2)
O(1)	0.049(2)	0.405(1)	0.2690(6)	9.1(6)
C(1)	0.106(2)	0.360(2)	0.3158(8)	5.3(6)
N(11)	0.314(1)	0.1861(9)	0.4815(5)	3.3(4)
C(12)	0.467(2)	0.223(1)	0.5081(7)	4.5(5)
C(13)	0.538(2)	0.165(2)	0.5665(8)	5.0(6)
C(14)	0.457(2)	0.069(2)	0.5975(7)	5.6(7)
C(15)	0.299(2)	0.026(1)	0.5667(8)	4.9(6)
C(16)	0.232(2)	0.089(1)	0.5112(7)	4.2(5)
N(21)	-0.107(2)	0.716(1)	0.3086(8)	19(1)
C(22)	-0.254(2)	0.665(1)	0.2751(8)	7.1(4)
C(23)	-0.358(2)	0.579(1)	0.3087(8)	6.2(4)
C(24)	-0.316(2)	0.544(1)	0.3757(8)	5.5(4)
C(25)	-0.170(2)	0.595(1)	0.4093(8)	5.7(4)
C(26)	-0.065(2)	0.681(1)	0.3757(8)	13.1(8)

and 2.079(3) Å][4]; 4-M-ImH[*trans*-$RuCl_4$(4-M-Im)$_2$] [2.364(2) and 2.087(6) Å][4] and M-ImH[*trans*-$RuCl_4$(CO)(M-Im)] (M-Im = 1-methylimidazole) [2.348(2) and 2.126(6) Å][7]. The Ru-N distances present in the above mentioned carbonyl complexes reflect the backbonding of the Ru-CO interactions, making the Ru-N length slightly longer when compared with those found for the related pyH[*trans*-$RuCl_4(py)_2$], ImH[*trans*-$RuCl_4(Im)_2$] and 4-M-ImH[*trans*-$RuCl_4$(4-M-Im)$_2$] compounds. The Ru-C distance for the complex (**2**) [1.87(2) Å] can be appropriately compared with those of M-ImH[*trans*-$RuCl_4$(CO)(M-Im)] [1.869(9) Å][7]. It is interesting to note that the species 4-NO_2Im[$RuCl_4$(5-NO_2Im)$_2$] was reported to show similar bond distances found for the crystal structures of the Ru(III) complexes mentioned above[15].

The strong absorption band in the IR spectrum at 2044 cm^{-1} corresponding to the $\nu_{(CO)}$ stretch, is shifted with respect to the free CO absorption band at 2143 cm^{-1} [16], indicating a small amount of metal-CO backbonding. The same behavior was found for the M- ImH[*trans*-$RuCl_4$(CO)(M-Im)] [7] complex where $\nu_{(CO)}$ is 2037 cm^{-1}. The Ru-Cl stretching frequencies were also observed, at 316 cm^{-1} and 328 cm^{-1} for the complexes (**1**) and (**2**), respectively.

The electronic absorption spectra for the complexes with the pyridine ligands are similar to the complex with the methylimidazole ligand[7] and show three bands:(**1**) 360 (ε = 1180 M^{-1} cm^{-1}), 441 (ε = 3200 M^{-1} cm^{-1}) and 532 nm (ε = 400 M^{-1} cm^{-1}); (**2**) 315(ε = 1150 M^{-1} cm^{-1}), 442 (ε = 3170 M^{-1} cm^{-1}) and 530 nm(ε = 390 M^{-1} cm^{-1}). The two higher energy transitions for these complexes can be assigned as ligand-to-metal charge transfer (LMCT) transitions. On the basis of the observed C_{4v} symmetry of the complexes (**1**) and (**2**), the bands at lower energies can be tentatively assigned to the d-d transitions $^1A_1 \rightarrow {}^1B_2$, according to the energy-levels proposed by Bacci and coworkers[17].

The EPR spectra of the complexes measured at X band and -150 °C show axial symmetries in the structures with $g_\perp$ = 2.2591(3) and 2.2585(3) and $g_\parallel$ =1.9431(3) and 1.9433(3), for compound (**1**) and (**2**), respectively.

The solution μ_{eff} values for the complexes (1) and (2) yielded spin-only values close to 1.7 μ_B being consistent with one unpaired electron per atom of ruthenium. The molar conductivity data obtained for these complexes in nitromethane, close to 70 Ω^{-1} cm^2 mol^{-1}, is consistent with 1:1 electrolytes[18].

Acknowledgments

We thank FAPESP, CAPES, CNPq and FINEP for financial support of this work.

References

1. Sigel, H. *Met. Ions Biol. Syst.* **1980**, 11.
2. Farrell N. In *Transition Metal Complexes as Drugs and Chemotherapeutic Agents*, Kluwer Academic Publishers, Boston, 1989, Ch. 6, pp. 147-151.
3. Clarke, M.J. In *Metal Complexes in Cancer Chemotherapy*, Keppler, B.K., Ed., VCH, Weinheim, Germany, 1993, Ch. 7, pp. 179-186
4. Keppler, B.K.; Rupp, W.; Juhl, U.M.; Endres, H.; Niebl, R.; Balzer, W. *Inorg. Chem*. **1987**, *26*, 4366.
5. Keppler, B.K.; Henn, M.; Juhl, U.M.; Berger, M.R.; Niebl, R.; Wagner, F.E. *Prog. Clin. Biochem. Med*. **1989,** *10*, 41.
6. Keppler, B.K.; Lipponer, K.G.; Stenzel, B.; Kratz, F. In *Metal Complexes in Cancer Chemotherapy*, Keppler, B.K., Ed., VCH, Weinheim, Germany, 1993, Ch. 9, pp. 187-220.
7. Batista, A.A.; Olmo, L.R.; V. Oliva, G.; Castellano, E.E.; Nascimento, O.R. *Inorg. Chim. Acta*. **1992,** *202*, 37.
8. Stephenson, T.A.; Wilkinson, G. *J. Inorg. Nucl. Chem*. **1966**, *28*, 945.
9. Walker, N.; Stuart, D. *Acta Cryst*. **1983,** A39, 158.
10. Sheldrick, G.M. SHELX-76. Program for Crystal Structure Determination Univ. of Cambridge, England, 1976.
11. Cromer, D.T; Liberman, D. *J.Chem. Phys*. **1970**, *53*, 1891.
12. Cromer, D.T.; Mann, J.B. *Acta Cryst*. **1968**, A24, 321.
13. Johnson, C.K. ORTEP. Report ORNL-3794, Oak Ridge National Laboratory, Tennessee,USA, 1965.
14. Evans, D.F. *J.Chem. Soc*. **1959**, 2003.
15. Anderson, C.; Beauchamp, A.L. *Inorg. Chim. Acta*. **1995**, *233*, 33.
16. Elschenbroich, Ch.; Salzer, A. In *Organometallics - A Concise Introduction*, VCH, Weinheim, Germany, 1989, p. 229.
17. Bacci, M.; Midollini S.; Stoppioni, P.; Sacconi. L. *Inorg. Chem*. **1973**, *12*, 1801.
18. Geary, W.J. *Coord. Chem. Rev*. **1971**, *7*, 81.

FAPESP helped in meeting the publication costs of this article